

Covalent binding of ATP $\gamma$ S to the nucleotide-binding site in S14C-actin<sup>1</sup>Herwig Schüler<sup>a</sup>, Clarence E. Schutt<sup>b</sup>, Uno Lindberg<sup>a</sup>, Roger Karlsson<sup>a,\*</sup><sup>a</sup>Department of Cell Biology, The Wenner-Gren Institute, Stockholm University, S-106 91 Stockholm, Sweden<sup>b</sup>The Henry Hoyt Laboratory, Department of Chemistry, Princeton University, Princeton, NJ, USA

Received 19 April 2000; received in revised form 30 May 2000

Edited by Matti Saraste

**Abstract** We have recently reported on the characterization of  $\beta$ -actin carrying the mutation S14C in one of the phosphate-binding loops. The present paper describes the attachment of the adenosine 5'-[gamma-thio]-triphosphate (ATP $\gamma$ S) to actin containing this mutation. Treatment of S14C-actin with ATP $\gamma$ S blocked further nucleotide exchange and raised the thermal stability of the protein, suggesting the formation of a covalent bond between the sulfhydryl on the terminal phosphate of ATP $\gamma$ S and cysteine-14 of the mutant actin. The affinity of the derivatized G-actin for DNase I as compared to wild-type ATP-actin was lowered to a similar extent as that of ADP·AlF<sub>4</sub>-actin. The derivatized actin polymerized slower than ATP-actin but faster than ADP-actin. Under these conditions the bound ATP $\gamma$ S was hydrolyzed, suggesting the formation of a state corresponding to the transient ADP·P<sub>i</sub>-state. ATP $\gamma$ S-actin interacted normally with profilin, whereas the interaction with actin depolymerizing factor (ADF) was disturbed, as judged on the effects of these proteins on actin polymerization. © 2000 Federation of European Biochemical Societies. Published by Elsevier Science B.V. All rights reserved.

**Key words:** ATP $\gamma$ S; cysteine reactivity; Non-exchangeable nucleotide; DNase I affinity; Yeast-expressed non-muscle actin; Polymerization

## 1. Introduction

Actin filaments (F-actin) are the major component of microfilaments, one of the force-generating systems of eukaryotic cells. Hydrolysis of ATP accompanies assembly of actin monomers (G-actin) into filaments, and turnover of the actin nucleotide is crucial for microfilament dynamics [1–3]. The molecular mechanisms of the ATPase reaction and its consequences for the functioning of the actin molecule are poorly understood. Actin has a higher affinity for ATP than for a number of other nucleotides and nucleotide analogs [4], and the protein is unstable when the nucleotide-binding site is unoccupied [5]. Therefore, it has been difficult to obtain actin preparations with bound non-hydrolyzable nucleotide analogs devoid of ATP-bound and denatured actin. A solution to

these problems is to attach nucleotide analogs covalently to the active site. This technique was successfully used to identify catalytic residues in different enzymes, locking them in their enzymatic cycle (see [6,7] for reviews).

Previously, covalent attachment of nucleotide analogs to actin was conducted to block the polymerization reaction in order to obtain a crystallizable form of actin [8,9], and to map the nucleotide-binding site [10,11]. In the light of recent progress in microfilament turnover (reviewed by [3]), it is worthwhile to reexamine such nucleotide analogs as tools for studying the role and mechanism of the actin ATPase.

Actin has been shown to bind and hydrolyze ATP $\gamma$ S [12]. Recently, a cysteine was introduced in close proximity of the  $\gamma$ -phosphate of the actin-bound ATP by site-directed mutagenesis [13]. The results presented here indicate that ATP $\gamma$ S becomes covalently coupled to this mutant  $\beta$ -actin.

## 2. Materials and methods

### 2.1. Chemicals

Bovine pancreatic DNase I (crystalline) was from Chemicon ICN. Hydroxyapatite (even lot number) was from Clarkson Chromatography Products (South Williamsport, PA, USA). Rhodamine-phalloidin,  $\epsilon$ ATP, and *N*-(1-pyrene)iodoacetamide were from Molecular Probes (Eugene, OR, USA). ADP $\beta$ S and ATP $\gamma$ S were from Aldrich-Sigma.

### 2.2. Mutagenesis and protein purification

Mutagenesis of the chicken  $\beta$ -actin gene, expression in *Saccharomyces cerevisiae*, and isolation of the mutant  $\beta$ -actins followed previously published protocols [13,14]. Recombinant  $\beta$ -actin was kept in G-buffer (5 mM Tris-HCl, pH 7.6, 0.5 mM ATP, 0.1 mM CaCl<sub>2</sub>, 0.5 mM DTT, 0.006% NaN<sub>3</sub>). ADP-actin was prepared by a cycle of polymerization/depolymerization and subsequent gel filtration on Sephacryl S-300 (Pharmacia) in G-buffer containing 0.5 mM ADP instead of ATP. Exchange of the high-affinity Ca<sup>2+</sup> for Mg<sup>2+</sup> was achieved by incubating actin in G-buffer with 0.2 mM EGTA and 50  $\mu$ M MgCl<sub>2</sub> for 15 min at room temperature [15]. For AlF<sub>4</sub> treatment, 0.1 mM Al(NO<sub>3</sub>)<sub>3</sub> and 0.5 mM NaF were added to monomeric ADP-actin. Profilin and  $\beta/\gamma$ -actin were purified from bovine thymus [16]. *Arabidopsis thaliana* ADF1 was expressed in *Escherichia coli* and purified according to [17]. All experiments were conducted at 25°C.

### 2.3. Reaction of ATP $\gamma$ S with S14C-actin

Excess nucleotide and DTT were removed from S14C-actin by gel filtration on Sephadex G-25 (Pharmacia), ATP $\gamma$ S was added from a stock solution (pH 7.4) to a final molar ratio of 10:1 over actin, and the samples were incubated at room temperature. Covalent attachment of ATP $\gamma$ S to S14C-actin was complete after 10 min, as judged by completely blocked nucleotide exchange (see Section 3).

To verify covalent attachment of the nucleotide to S14C-actin, the reaction was performed using ATP $\gamma$ [<sup>35</sup>S] (Amersham) at a final activity of 50  $\mu$ Ci/ml. Part of the reaction mixture was cleaved with trypsin (sequencing grade) at a molar ratio of 1:100 over actin for 2 h at 15°C. The samples were mixed with 0.2 vol of non-reducing sample buffer (50 mM Tris-HCl pH 7.6, 10% glycerol, 0.2% SDS), denaturing electrophoresis was performed in 18% acrylamide gels, and fixed gels were autoradiographed.

\*Corresponding author. Fax: (46)-8-159837.

E-mail: roger.karlsson@cellbio.su.se

<sup>1</sup> Enzyme: DNase I, deoxyribonuclease I (EC 3.1.21.1).

**Abbreviations:** *A*<sub>cc</sub>, critical concentration for actin polymerization; ADP $\beta$ S, adenosine 5'-[beta-thio]-diphosphate; ATP $\gamma$ S, adenosine 5'-[gamma-thio]-triphosphate;  $\epsilon$ ATP, 1,*N*<sup>6</sup>-ethenoadenosine 5'-triphosphate

#### 2.4. Thin layer chromatography

F-actin pellets were dissolved in 0.3 M perchloric acid and spotted onto PEI-cellulose sheets (Merck). Ascending chromatography was performed in 0.5 M formic acid, 1 M LiCl<sub>2</sub> after which the cellulose sheets were examined under UV light [18].

#### 2.5. DNase I-actin interaction

The actin:DNase I interaction was studied using the DNase I-inhibition assay [19] and the affinity of the complex was determined from double-reciprocal plots of the DNase I-inhibition activity as a function of actin concentration.

#### 2.6. Nucleotide exchange

After addition of  $\epsilon$ ATP [20] to G-actin (10  $\mu$ M) in the presence of different nucleotides, the fluorescence increase at  $>408$  nm (excitation at 360 nm) was monitored using a Sigma ZWS II spectrofluorimeter (Biochem Wissenschaftliche Geräte GmbH, Puchheim, Germany).

#### 2.7. Thermal denaturation of actin

The DNase I-inhibition assay [19] was used to assess the thermal stability of actin, as described in [21]. The  $T_m$  was defined as the temperature at which 50% of the initial DNase I-inhibition activity, measured at 25°C, was lost.

#### 2.8. Actin polymerization

Filament formation was monitored by the increase in fluorescence due to copolymerization of 2% pyrene-labeled bovine  $\beta/\gamma$ -actin [22] as described [13]. The critical concentration for polymerization ( $A_{cc}$ ) was estimated using the sedimentation/DNase I-inhibition assay [13].

### 3. Results and discussion

#### 3.1. Reaction of ATP $\gamma$ S with S14C-actin

In the tight state of actin, the S14-hydroxyl is within hydrogen bonding distance of the  $\gamma$ -phosphate of ATP (Fig. 1) [23,24]. Therefore,  $\beta$ -actin carrying the mutation S14C [13] provided the possibility of attaching cysteine-reactive nucleotides to the nucleotide-binding site. The cysteic side chain is somewhat larger than the wild-type seryl side chain. Therefore, the sulfhydryl groups of either ADP $\gamma$ S or ATP $\gamma$ S were candidates for forming a disulfide with cysteine-14 of the mutant actin.

The results in Fig. 2A show that incubation of S14C-actin in the presence of ATP $\gamma$ S blocked incorporation of the fluorescent nucleotide  $\epsilon$ ATP. In contrast, ATP and ADP $\gamma$ S were readily replaced by  $\epsilon$ ATP. Therefore it was concluded that ATP $\gamma$ S was covalently attached to cysteine-14 of the mutant actin. Addition of 10 mM DTT only led to a slow increase of

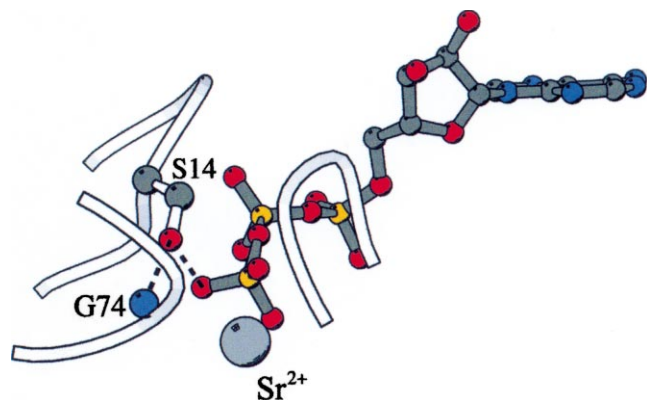


Fig. 1. Schematic detail of the nucleotide-binding site of  $\beta$ -actin (pdb access code 2btff). The hydroxyl of serine-14, in the phosphate-binding loop of actin subdomain 1, is within hydrogen-bonding distance of the  $\gamma$ -phosphate of ATP and the backbone amide of glycine-74. The figure was prepared using MolScript [41].

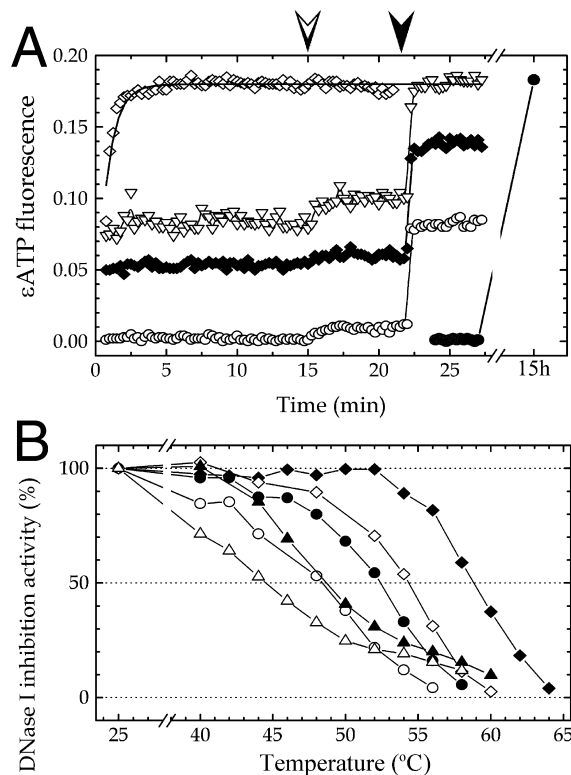


Fig. 2. ATP $\gamma$ S bound to monomeric S14C-actin is inexchangeable. A: Mg-actin (10  $\mu$ M) carrying the S14C replacement was incubated with 0.1 mM of either ATP $\gamma$ S (circles), ADP $\gamma$ S (triangles), ATP (filled diamonds), or in the absence of nucleotide (open diamonds). The fluorescence increase was monitored after addition of 0.1 mM  $\epsilon$ ATP. The open arrowhead indicates addition of 10 mM DTT, and the solid arrowhead indicates addition of  $\epsilon$ ATP to 0.5 mM. Closed circles represent a separate experiment where 0.1 mM  $\epsilon$ ATP and 1 mM DTT were added to ATP $\gamma$ S-actin and the incubation was performed overnight. B: The loss of DNase I-inhibition activity in solutions of Mg-actin (open symbols) or Ca-actin (filled symbols) during heating at a rate of 40°C/h. The bound ATP $\gamma$ S (circles) considerably stabilized S14C-actin, manifested as a shift of  $T_m$  by approximately 4°C compared to ATP conditions (triangles). For comparison, the melting curves for wild-type ATP-actin are also shown (diamonds).

$\epsilon$ ATP fluorescence. Additional  $\epsilon$ ATP added to ATP $\gamma$ S-actin caused an increase in fluorescence to 40% of the final level of the control (Fig. 2A, open circles and open diamonds), as compared to 80% when added to ATP-actin (filled diamonds). Thus, apparently the cysteine-14–ATP $\gamma$ S disulfide was shielded from reduction by DTT. Only after prolonged incubation (15 h) with 1 mM DTT the fluorescence signal was restored to a level indicating full incorporation of  $\epsilon$ ATP.

The intrinsically unstable S14C-actin was significantly stabilized by ATP $\gamma$ S, regardless of whether Mg<sup>2+</sup> or Ca<sup>2+</sup> was bound at the high-affinity cation-binding site. The melting temperature of the mutant actin, measured using the DNase I-inhibition assay [21], was increased approximately 4°C by ATP $\gamma$ S (Fig. 2B). This supports the interpretation that the nucleotide becomes covalently attached to the protein. While wild-type actin denatures with first-order kinetics, S14C-actin does not [13]. The derivatization of the mutant actin normalized its denaturation kinetics. The stabilization was unaffected by DTT (10 mM), confirming the inaccessibility of the formed bond for the reducing agent.

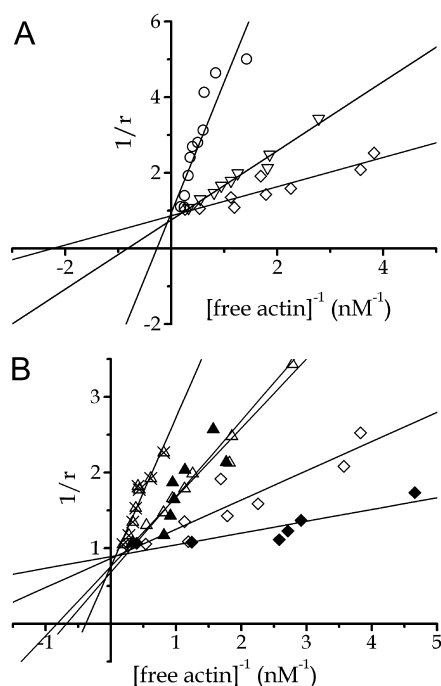


Fig. 3. The ligands in the actin interdomain cleft affect DNase I binding, and ATP $\gamma$ S-S14C-actin and ATP·AlF $_4$ -actin have similar affinities for DNase I. Double-reciprocal plots of the actin concentration-dependent inhibition of DNase I, where  $r = [\text{bound actin}]/[\text{DNase I}]$ . A: Mg-ATP-actin (diamonds), Mg-ADP-actin (triangles), and Mg-ATP $\gamma$ S-S14C-actin (circles). B: Ca- and Mg-ATP-actin (filled and open diamonds, respectively), Ca- and Mg-ADP-actin (filled and open triangles, respectively), and Mg-ADP·AlF $_4$ -actin (crossed triangles). The dissociation constants determined from these plots are summarized in Table 2.

### 3.2. Conformation of ATP $\gamma$ S-actin

To probe the conformation of the derivatized actin, its affinity for DNase I was studied. The results showed that DNase I bound to the Mg form of ATP $\gamma$ S-actin with lower affinity than to either ATP- or ADP-actin (Fig. 3A and Table 1). This prompted the investigation of the effects of different ligands bound to the interdomain cleft on the actin:DNase I interaction. As shown in Fig. 3B, also AlF $_4$  binding to ADP-actin weakened the DNase I interaction significantly. In addition, DNase I binding is sensitive to both the actin-bound nucleotide and divalent cation.

Hydrolysis of ATP $\gamma$ S by actin and other ATPases has been observed before (e.g. [25,26]). To investigate whether the  $\gamma$ -phosphate bond of ATP $\gamma$ S was available for hydrolysis by S14C-actin, the derivatized actin was incubated under polymerizing conditions (see below) overnight at room tempera-

Table 1

Effect of the nucleotide and the high-affinity divalent cation on the affinity of the actin–DNase I complex

	Mg-actin	Ca-actin
ATP-actin	0.44 $\pm$ 0.07	0.18 $\pm$ 0.04
ATP $\gamma$ S-actin	3.63 $\pm$ 0.56	n.d.
ADP·AlF $_4$ -actin	2.60 $\pm$ 0.36	n.d.
ADP-actin	1.22 $\pm$ 0.08	1.47 $\pm$ 0.34

The  $K_d$  values (in nM) for the actin–DNase I interaction were determined using the DNase I-inhibition assay. Values represent means  $\pm$  S.D. of the values determined by linear curve fits from the plots shown in Fig. 3.

ture. Thin layer chromatography of the nucleotide extracted from the protein demonstrated the presence of exclusively ADP in the F-actin. Thus, ATP $\gamma$ S had been hydrolyzed. It is generally believed that the binding of AlF $_4$  to an ATPase captures the protein in a transition state resembling the ADP·P $_i$ -state in the nucleotide hydrolysis reaction [27]. Since the ATP $\gamma$ S-G-actin resembled the ADP·AlF $_4$ -bound state with

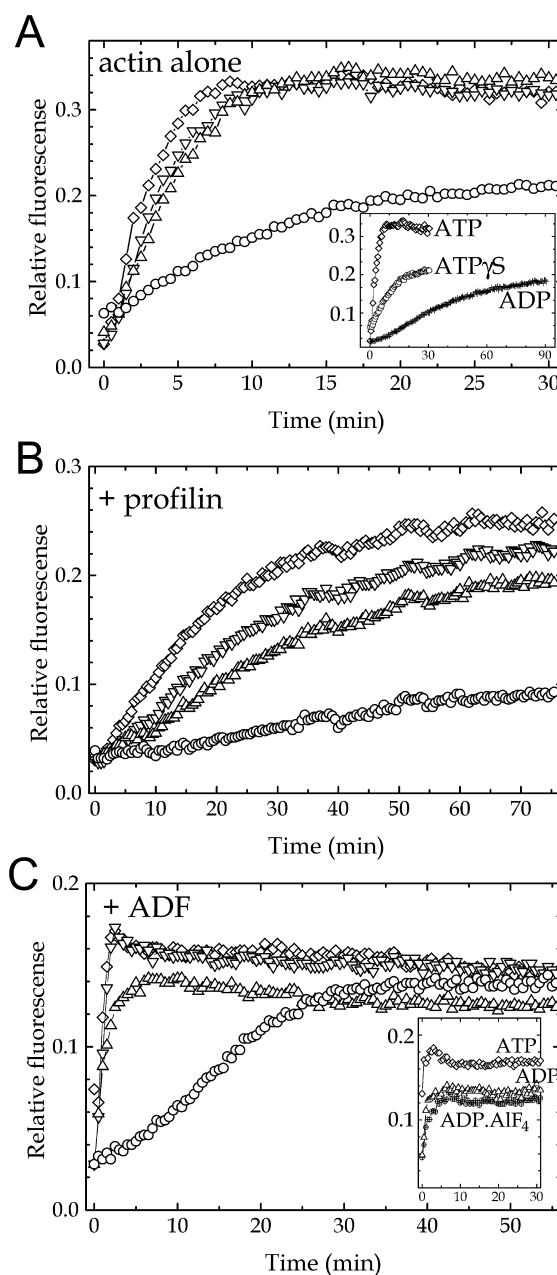


Fig. 4. ATP $\gamma$ S-S14C-actin is disturbed in its polymerization kinetics and binding to ADF. Panel A: Increase in pyrenyl fluorescence during filament formation, induced by addition of 1 mM MgCl $_2$ +100 mM KCl to 8  $\mu$ M ATP-actin alone (diamonds), ATP-actin containing 5% (down triangles) or 20% ATP $\gamma$ S-S14C-actin (up triangles), and 8  $\mu$ M ATP $\gamma$ S-S14C-actin alone (circles). The inset shows the polymerization of Mg-ADP-actin for comparison ('crosses'). Panel B: As in A but after preincubation with equimolar amounts of profilin. Panel C: As in A but after preincubation with equimolar ADF. Inset: Polymerization of ATP-, ADP·AlF $_4$ -, and ADP-actins (diamonds, crossed circles, and triangles, respectively) in complex with ADF.

respect to DNase I binding, it is plausible that the F-actin is trapped in the ADP.P<sub>i</sub>-state.

### 3.3. Polymerizability of ATPγS-actin, and its interaction with profilin and ADF

The S14C-mutation per se did not notably affect the polymerization properties of the protein under physiological salt conditions (1 mM MgCl<sub>2</sub>+100 mM KCl) [13]. The ATPγS-actin polymerized more slowly than wild-type ATP-actin, but faster than ADP-actin (Fig. 4A), and the final level of polymerization with ATPγS-actin was lowered. The *A<sub>cc</sub>* for ATPγS-actin was more than three times higher than for wild-type ADP-actin and almost 10 times higher than for ATP-actin (Table 2). Copolymerization of ATP-actin with 5 or 20% ATPγS-actin barely affected the polymerization kinetics, showing that the cooperativity within the actin filament could overcome the polymerization defects of the derivatized actin. Equimolar phalloidin or rhodamine–phalloidin reduced the *A<sub>cc</sub>* of the derivatized actin by a factor of 5 (Table 2) and accelerated its polymerization (not shown). Thus, phalloidin could normalize the polymerizability of the derivatized actin. A similar effect of phalloidin was seen earlier in the case of polymerization deficient, partially digested [28,29] and site specifically mutated actins [30].

Profilin and the ADF/cofilin proteins are modulators of actin dynamics (see [3] for a recent review). The ADF/cofilins bind G-actin preferentially in its ADP-bound form [31]. While several observations suggest that profilin binds ATP-actin more tightly [32,33], other indicate similar profilin binding to ATP- and ADP-actin [34,35].

Profilin clearly interfered with the de novo filament formation from both ATP-actin and ATPγS-actin (compare Fig. 4A and B). Equimolar amounts of profilin added to F-actin formed from ATP-actin, from ATP-actin copolymerized with 5 or 20% ATPγS-actin, or from ATPγS-actin led to a 30% decrease in pyrenyl fluorescence, with similar kinetics in all four cases, and new steady-state levels were established within 30 min (not shown). Profilin also decreased the steady-state levels of sedimentable ATPγS-, ATP- and ADP-actins (Table 2). However, here the sequestering effect of profilin on the derivatized actin was smaller than expected from the results obtained with the pyrenyl assay (Fig. 4B). This could be due to a lower affinity of profilin for pyrenyl-actin [36,37], or to a difference in the mechanical stabilities of wild-type and mutant actin filaments (see also [13]).

The presence of ADF greatly accelerated the polymerization of ATP-actin and decreased the final levels of filamentous

actin (Fig. 4C). This may be explained by enhanced nucleation in the presence of ADF [17,38,39], and an increased dissociation rate due to ADF also binding to filamentous actin [17,40]. Also when ATP-actin was copolymerized with increasing concentrations of ATPγS-actin (Fig. 4C), ADF increased the rate of polymer formation, and lowered the steady-state level of fluorescence. However, ADF did not affect the level of sedimentable ATPγS-actin (Table 2). It is known that ADF/cofilin proteins bind only weakly to the ADP.P<sub>i</sub>-conformation of F-actin [40]. However, ADF nucleated the polymerization of ATP-, ADP- and ADP.AIF<sub>4</sub>-actins to a similar extent (inset Fig. 4C). Thus, the lack of effect of ADF on the final level of polymerization of derivatized actin may be explained by an ADP.P<sub>i</sub>-actin-like conformation of the filaments or by a disturbance in their ability to release inorganic phosphate.

In summary, this paper presents evidence that ATPγS binds covalently to S14C-actin, and that ligand binding in the central cleft modulates the affinity of actin for DNase I. The derivatized protein behaved like ADP.P<sub>i</sub>- and ADP.AIF<sub>4</sub>-actin in its binding to DNase I suggesting it to be a valuable tool for studying the role of ATP hydrolysis by actin, and the formation of F-ADP.P<sub>i</sub> with the P<sub>i</sub> covalently bound to the actin protomers could be useful for further studies on the formation of the actin filament and its structure.

**Acknowledgements:** We thank Greg Bowman for providing *A. thaliana* ADF1, and Nam-Hai Chua for the *At*ADF1 cDNA. We acknowledge financial support from the Swedish National Research Council (NFR) to U.L. and R.K., from the Swedish Foundation for International Cooperation in Research and Higher Education (STINT) to U.L., and from the NIH (GM44038) to C.E.S.

## References

- [1] Theriot, J.A. (1994) Adv. Exp. Med. Biol. 358, 133–145.
- [2] Carlier, M.F. and Pantaloni, D. (1997) J. Mol. Biol. 269, 459–467.
- [3] Chen, L., Bernstein, B.W. and Bamberg, J.R. (2000) Trends Biochem. Sci. 25, 19–23.
- [4] Waechter, F. and Engel, J. (1977) Eur. J. Biochem. 74, 227–232.
- [5] Asakura, S. (1961) Arch. Biochem. Biophys. 92, 140–149.
- [6] Fukui, T. (1995) J. Biochem. 117, 1139–1144.
- [7] Sprang, S.R. (1997) Curr. Opin. Struct. Biol. 7, 849–856.
- [8] Faust, U., Fasold, H. and Ortanderl, F. (1974) Eur. J. Biochem. 43, 273–279.
- [9] Bender, N., Fasold, H. and Rack, M. (1974) FEBS Lett. 44, 209–212.
- [10] Hegyi, G., Szilagyi, L. and Elzinga, M. (1986) Biochemistry 25, 5793–5798.
- [11] Kuwayama, H., Miki, M. and dos Remedios, C.G. (1989) FEBS Lett. 250, 328–330.
- [12] Mannherz, H.G., Brehme, H. and Lamp, U. (1975) Eur. J. Biochem. 60, 109–116.
- [13] Schüler, H., Korenbaum, E., Schutt, C.E., Lindberg, U. and Karlsson, R. (1999) Eur. J. Biochem. 265, 210–220.
- [14] Karlsson, R. (1988) Gene 68, 249–257.
- [15] Gershman, L.C., Newman, J., Selden, L.A. and Estes, J.E. (1984) Biochemistry 23, 2199–2203.
- [16] Lindberg, U., Schutt, C.E., Hellsten, E., Tjader, A.C. and Hult, T. (1988) Biochim. Biophys. Acta 967, 391–400.
- [17] Carlier, M.F. et al. (1997) J. Cell Biol. 136, 1307–1322.
- [18] Neidl, C. and Engel, J. (1979) Eur. J. Biochem. 101, 163–169.
- [19] Blikstad, I., Markey, F., Carlsson, L., Persson, T. and Lindberg, U. (1978) Cell 15, 935–943.
- [20] Secrist, J.A., Barrio, J.R., Leonard, N.J., Villar-Palasi, C. and Gilman, A.G. (1972) Science 177, 279–280.
- [21] Schüler, H., Lindberg, U., Schutt, C.E. and Karlsson, R. (2000) Eur. J. Biochem. 267, 476–486.

Table 2

Effect of covalently attached nucleotide on the critical concentrations for filament formation (*A<sub>cc</sub>*) in the presence of different ligands

Ligands added	ATP-actin	ATPγS-actin	ADP-actin
(No additives)	0.32 ± 0.03	3.02 ± 0.2	0.92 ± 0.08
Phalloidin	0.18	0.59 ± 0.32	0.25 ± 0.11
Profilin	2.54 ± 0.11	4.12 ± 0.29	3.86 ± 0.82
ADF	2.72 ± 0.08	3.01 ± 0.21	7.0 ± 0.04

Monomeric Mg-actin (8 μM) was preincubated with an equimolar amount of the respective ligands for 5 min before incubation with 1 mM Mg<sup>2+</sup>+0.1 M K<sup>+</sup> for 3 h. Actin filaments were sedimented by ultracentrifugation, and the *A<sub>cc</sub>* was determined in the supernatants using the DNase I-inhibition assay. Values for *A<sub>cc</sub>* are given in μM and represent means ± S.D. of three to six determinations.

- [22] Kouyama, T. and Mihashi, K. (1981) *Eur. J. Biochem.* 114, 33–38.
- [23] Kabsch, W., Mannherz, H.G., Suck, D., Pai, E.F. and Holmes, K.C. (1990) *Nature* 347, 37–44.
- [24] Schutt, C.E., Myslik, J.C., Rozycki, M.D., Goonesekere, N.C. and Lindberg, U. (1993) *Nature* 365, 810–816.
- [25] Yu, X. and Egelman, E.H. (1992) *J. Mol. Biol.* 225, 193–216.
- [26] Van Dijk, J., Fernandez, C. and Chaussepied, P. (1998) *Biochemistry* 37, 8385–8394.
- [27] Wittinghofer, A. (1997) *Curr. Biol.* 7, R682–R685.
- [28] Higashi-Fujime, S., Suzuki, M., Titani, K. and Hozumi, T. (1992) *J. Biochem. (Tokyo)* 112, 568–572.
- [29] Kiessling, P., Jahn, W., Maier, G., Polzar, B. and Mannherz, H.G. (1995) *Biochemistry* 34, 14834–14842.
- [30] Kuang, B. and Rubenstein, P.A. (1997) *J. Biol. Chem.* 272, 1237–1247.
- [31] Maciver, S.K. and Weeds, A.G. (1994) *FEBS Lett.* 347, 251–256.
- [32] Perelroizen, I., Carlier, M.F. and Pantaloni, D. (1995) *J. Biol. Chem.* 270, 1501–1508.
- [33] Vinson, V.K., De La Cruz, E.M., Higgs, H.N. and Pollard, T.D. (1998) *Biochemistry* 37, 10871–10880.
- [34] Perelroizen, I., Marchand, J.B., Blanchoin, L., Didry, D. and Carlier, M.F. (1994) *Biochemistry* 33, 8472–8478.
- [35] Selden, L.A., Kinoshian, H.J., Estes, J.E. and Gershman, L.C. (1999) *Biochemistry* 38, 2769–2778.
- [36] Malm, B. (1984) *FEBS Lett.* 173, 399–402.
- [37] Kang, F., Purich, D.L. and Southwick, F.S. (1999) *J. Biol. Chem.* 274, 36963–36972.
- [38] Nishida, E., Maekawa, S. and Sakai, H. (1984) *Biochemistry* 23, 5307–5313.
- [39] Hawkins, M., Pope, B., Maciver, S.K. and Weeds, A.G. (1993) *Biochemistry* 32, 9985–9993.
- [40] Blanchoin, L. and Pollard, T.D. (1999) *J. Biol. Chem.* 274, 15538–15546.
- [41] Kraulis, P.J. (1991) *J. Appl. Crystallogr.* 24, 946–950.